



## INDUCTION MOTOR WINDINGS FAULTS DETECTION USING FLUX-ERROR BASED MRAS ESTIMATORS

Szymon Antoni BEDNARZ, Mateusz DYBKOWSKI

Wrocław University of Science and Technology, Department of Electrical Machines, Drives and Measurements, Smoluchowskiego 19, 50-370, Wrocław, Poland  
[szymon.bednarz@pwr.edu.pl](mailto:szymon.bednarz@pwr.edu.pl); [mateusz.dybkowski@pwr.edu.pl](mailto:mateusz.dybkowski@pwr.edu.pl)

### Abstract

The paper is concerned with detection of a stator and rotor winding faults in a squirrel-cage induction motor. The idea of the fault detection is based on a hypothesis that each of windings faults results in a sharp increase or decrease of internal parameters' values of the machine, therefore it can be treated as a suitable fault symptom. Resistances of the stator and rotor windings seem to be adequate quantities due to their direct relationship with the machine windings. An observation and analysis of the parameters' changes in a real-time domain enables to an incipient detection of the fault. It is evident that internal parameters of the machine can't be measured directly during operation on the drive system thus the only way is an estimation by specialized algorithms. In the paper two estimators based on Model Reference Adaptive System (MRAS) were utilized to achieve this goal. Two simple algorithms for faults detection are proposed as well. Detailed description of fault detection systems is included in the paper. Proposed systems were tested on computer simulations performed by MATLAB/Simulink software. Then, experimental tests were carried out on the laboratory setup to confirm usefulness of proposed approaches.

Keywords: induction motor, stator fault, rotor fault, faults detection, parameter estimator, MRAS

### DETEKCJA USZKODZEŃ UZWOJEŃ SILNIKA INDUKCYJNEGO Z ZASTOSOWANIEM ESTYMATORÓW MRAS BAZUJĄCYCH NA BŁĘDZIE ESTYMACJI STRUMIENIA

#### Streszczenie

Artykuł skupia się na wykrywaniu wybranych uszkodzeń uzwojeń stojana i wirnika silnika indukcyjnego klatkowego. Idea detekcji opiera się na założeniu, że każde uszkodzenie uzwojeń powoduje gwałtowną zmianę wartości wewnętrznych parametrów maszyny, co może być uznane jako miarodajny symptom uszkodzenia. Najbardziej odpowiednimi parametrami wydają się być rezystancje stojana i wirnika ze względu na bezpośrednie powiązanie z uzwojeniami silnika. Obserwacja i analiza zmian wartości tych parametrów w czasie rzeczywistym umożliwia wykrycie uszkodzenia w jego wczesnym stadium. W trakcie pracy napędu nie ma możliwości pomiaru rezystancji uzwojeń, dlatego też jedynym sposobem na uzyskanie informacji o ich aktualnych wartościach jest estymacja z zastosowaniem wyspecjalizowanych algorytmów. W pracy do realizacji tego celu zastosowano układy adaptacyjne z modelem odniesienia (MRAS). Ponadto zaproponowano również dwa proste algorytmy detekcji uszkodzeń uzwojeń stojana i wirnika. W artykule przedstawiono przegląd literatury dotyczący wykrywania uszkodzeń silnika indukcyjnego z zastosowaniem estymatorów parametrów. Proponowane rozwiązanie zostało sprawdzone poprzez analizę symulacyjną przeprowadzoną w środowisku MATLAB/Simulink a także zweryfikowane na stanowisku eksperymentalnym.

Słowa kluczowe: silnik indukcyjny, uszkodzenie stojana, uszkodzenie wirnika, wykrywanie uszkodzeń, estymator parametrów, MRAS

## 1. INTRODUCTION

Electric drives with induction motors (IM) are basic components in various systems, such as electric and hybrid cars, trams, trains, metro, power plants and industrial machines [1].

During operation of any electrical drive, damage of its components can be occurred including sensors (electrical or mechanical), power electronics devices and the machine [2], [3]. Internal faults of the machine can be divided into mechanical and electrical [2], [4]. According to the

literature up to 40% of faults belong to the stator windings and about 10% to the rotor winding.

Other faults are related to the bearing and another machine's components [5], [3]. Stator windings damages are related to an insulation degradation, what causes interturn short-circuit (ITSC) within a coil, while broken rotor bars and end-rings are electrical faults in the cage of the IM [4]. Motor's winding faults have a negative impact on the operation of the drive, and they should be detected as soon as possible, to avoid further

degradation of the machine and enable a safety stop of the drive [4], [6], [5], [3].

Several diagnostics techniques related to stator and rotor windings faults have been developed.

One of the most popular method is the signal-based (SB) diagnostic procedure [4], [6]. This technique consists of an analysis of measured signals such as: current, voltage, electromagnetic flux, power, mechanical vibration, angular speed and temperature [7], [3]. The analysis is performed on time, frequency or time-frequency domains to extract specific symptoms which are related to the faults [4]. These methods often utilize signal analysis techniques, which are based on the Fast Fourier Transform (FFT), Short Time Fourier Transform (STFT), Wavelet Transform (WT), Hilbert Transform (HT) [6], [3] etc. To improve an effectiveness of the faults diagnosis, these methods are often supported by solutions based on artificial intelligence (AI) (artificial neural networks (ANN), fuzzy logic (FL)) [6], [3], [8].

Nowadays, it has become a standard, that IM's work in closed-loop control systems what enable to precise regulation of IM's electromagnetic torque or the angular speed [1], [7]. However, closed-loop control systems (including vector control algorithms) can compensate effects of windings faults, what complicates the extraction of the faults symptoms from measured signals (f. ex. Stator currents) [9], [10]. Several signal-based diagnostics methods for closed-loop control systems are developed and presented in papers [10], [11], [12], [13], [14], [15], [16].

Another approach to damages detection is the model-based (MB) fault diagnosis technique which in general relies on a mathematical model of the machine [4], [17], [18], [3]. One of these methods is based on hypothesis, that winding faults symptoms can be observed as changes (a sharp decrease/increase, oscillations) of values of the IM parameters [19], [20], [17]. This method requires an identification of the IM parameters during its operation. Several identification algorithms have been utilized in a context to the IM's stator or rotor windings faults diagnosis. They have based on: last square error minimization [20], Kalman Filter [22], [22], [23], [24], [25], [26], [27], nonlinear programming [21], state observers [23], [28], [29], Moving Horizon Estimation, [30], [31], genetic algorithm [31], Sparse grid optimization [32], trust-region and Broyden-Fletcher-Goldfarb-Shanno (TR-BFGS) technique [30], and Sliding Mode Observer [34].

Despite, that many identification algorithms have been tested in a context to the IM's fault detection, not all existing approaches have been taken into consideration. One of them are estimators based on Model Reference Adaptive System (MRAS), which are often utilized in the IM drives to calculate state variables and parameters of the machine [35], [36], [37].

Therefore, in this paper a Flux-error based MRAS estimators (F-MRAS) are used to the IM's parameters identification in order to rotor or stator faults detection. Two estimators are utilized: first one [38], [39] is used to the rotor resistance estimation while second [40], [41] is used to the stator resistance estimation. Estimated parameters are utilized in faults detection algorithms, which are based on two simple assumptions [39], [41]:

- first – connected with rotor windings faults – rupture of a rotor's bar(s) results in a sharp increase of the estimated rotor resistance;
- second – connected with stator windings faults – ITSC results in a sharp decrease of the estimated stator resistance.

Due to the fact, that values of both resistances are strongly dependent on windings temperature (heating or cooling process), proposed algorithms were tested also for this phenomenon.

Studies were performed in the closed-loop control system based on Direct Field Oriented Control (DFOC) structure.

In the paper results of computer simulation studies are shown which were carried out by MATLAB/Simulink software. Results of the experimental validation are presented as well.

## 2. MATHEMATICAL MODELS OF THE INDUCTION MOTOR AND DIRECT FIELD ORIENTED CONTROL STRUCTURE

During computer simulations, a mathematical model of the IM with possibility to tests the stator and rotor windings faults are necessary. In the paper two types of mathematical models were used which are described in the stationary reference frame ( $\alpha$ - $\beta$ ). The first model to the stator faults analysis, the second one for the rotor faults analysis. In this chapter the control structure is also presented.

### 2.1. Model of the induction motor for the stator windings faults

To the ITSC simulation, a model proposed in [30] was used.

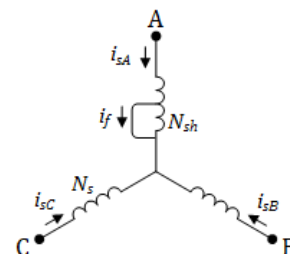


Fig. 1. ITSC in a phase A of the IM

It can be assumed [29], that the total number of turns in each phase is  $N_s$  and amount of shorted turns in  $N_{sh}$ . Relative number of shorted turns is  $\eta_f =$

$N_{sh}/N_s$ . Fig. 1 illustrates the scheme of the IM's stator windings with a short circuit in the phase A.

An electromagnetic flux connected with the faulted phase is given by:

$$T_N \frac{d\psi_f}{dt} = -r_s \mathbf{\mu}_{\alpha\beta}^T \mathbf{i}_s + \left( \mathbf{\mu}_{\alpha\beta} \left| r_s + r_f \right. \right) i_f, \quad (1)$$

where:  $r_s$  – stator windings resistance,  $r_f$  – shorted circuit resistance,  $i_f$  – shorted circuit current,  $\mathbf{i}_s$  – stator current vector,  $T_N = 1/(2\pi f_s N)$ ,  $\mathbf{\mu}_{\alpha\beta}$  is a modulus and  $\mu_\alpha, \mu_\beta$  are components of the vector  $\mathbf{\mu}_{\alpha\beta} = [\mu_\alpha, \mu_\beta]^T$  which indicate the fraction of the shorted turns and a phase of the short circuit respectively.

$$\mathbf{\mu}_{\alpha\beta|A} = \eta_{fA} \begin{bmatrix} 1 & 0 \end{bmatrix}^T, \quad (2)$$

$$\mathbf{\mu}_{\alpha\beta|B} = \eta_{fB} \begin{bmatrix} -\frac{1}{2} & \frac{\sqrt{3}}{2} \end{bmatrix}^T, \quad (3)$$

$$\mathbf{\mu}_{\alpha\beta|C} = \eta_{fC} \begin{bmatrix} -\frac{1}{2} & -\frac{\sqrt{3}}{2} \end{bmatrix}^T, \quad (4)$$

where:  $\eta_{fA}, \eta_{fB}, \eta_{fC}$  – relative amount of shorted turns for each phase.

The current in the short circuit can be obtain by equation:

$$i_f = \frac{\psi_f - \mathbf{\mu}_{\alpha\beta}^T \boldsymbol{\Psi}_s}{\left( \frac{2}{3} \left| \mathbf{\mu}_{\alpha\beta} \right|^2 - \left| \mathbf{\mu}_{\alpha\beta} \right| \right) x_{\sigma s}}, \quad (5)$$

where:  $\boldsymbol{\Psi}_s$  – stator flux vector,  $x_{\sigma s}$  – stator leakage reactance.

Stator and rotor fluxes are derived from voltage equations:

$$T_N \frac{d\boldsymbol{\Psi}_s}{dt} = \mathbf{u}_s - r_s \left( \mathbf{i}_s - \frac{2}{3} \mathbf{\mu}_{\alpha\beta} i_f \right), \quad (6)$$

$$T_N \frac{d\boldsymbol{\Psi}_r}{dt} = -r_r \mathbf{i}_r + j\omega_m \boldsymbol{\Psi}_r, \quad (7)$$

where:  $\mathbf{u}_s$  – stator voltage vector,  $\mathbf{i}_r$  – rotor voltage vector,  $\boldsymbol{\Psi}_r$  – stator flux vector,  $r_r$  – rotor windings resistance,  $\omega_m$  – angular rotor speed.

The other IM equations are given by:

$$\mathbf{i}_s = \frac{x_r}{w} \boldsymbol{\Psi}_s - \frac{x_m}{w} \boldsymbol{\Psi}_r + \frac{2}{3} \mathbf{\mu}_{\alpha\beta} i_f, \quad (8)$$

$$\mathbf{i}_r = \frac{x_s}{w} \boldsymbol{\Psi}_r - \frac{x_m}{w} \boldsymbol{\Psi}_s, \quad (9)$$

$$T_E = \text{Im} \left( \boldsymbol{\Psi}_s^* \left( \mathbf{i}_s - \frac{2}{3} \mathbf{\mu}_{\alpha\beta} i_f \right) \right), \quad (10)$$

$$\frac{d\omega_m}{dt} = \frac{1}{T_m} (T_E - T_L), \quad (11)$$

where:  $T_E$  – electromagnetic torque,  $T_L$  – load torque,  $x_s, x_r, x_m$  – stator, rotor, mutual reactance, respectively,  $T_m$  – mechanical constant.

## 2.2. Model of the induction motor for the rotor windings faults

To the rotor bars damage simulation, the model proposed in [41] was used. This model assumes that

a rupture of each of the rotor's bar results in an increase of the rotor resistance value. Rotor resistance components in  $\alpha\beta$  coordinates system are obtained by:

$$r_{r\alpha} = \frac{N_b r_{rN}}{2 \sum_{k=1}^{N_b} \mathbf{G}_w(k) \sin^2 \left( \theta + \frac{2\pi k}{N_b} \right)}, \quad (12)$$

$$r_{r\beta} = \frac{N_b r_{rN}}{2 \sum_{k=1}^{N_b} \mathbf{G}_w(k) \sin^2 \left( \theta + \frac{2\pi k}{N_b} - \frac{\pi}{2} \right)}, \quad (13)$$

where:  $N_b$  – number of rotor bars,  $\theta$  – angle of rotor position,  $\mathbf{G}_w$  – vector of rotor bars conductance, where each element corresponds to rotor bar condition (if  $\mathbf{G}_w(k) = 0$  – faulted,  $\mathbf{G}_w(k) = 1$  – healthy).

Rotor resistance components calculated by (12-13) are used in the rotor voltage equation (7) instead of the constant  $r_r$  parameter. When  $N_b = 0$  rotor resistance components are equal to the nominal value of this quantity. During rotor bars faults obtained rotor resistance components oscillate, what results in stator currents modulation.

## 2.3. Direct Field Oriented Control Structure

In the paper, proposed fault detection systems were tested in the closed-loop control system of the IM. During studies the Direct Field Oriented Control (DFOC) algorithm was utilized, which diagram is illustrated in Fig. 2.

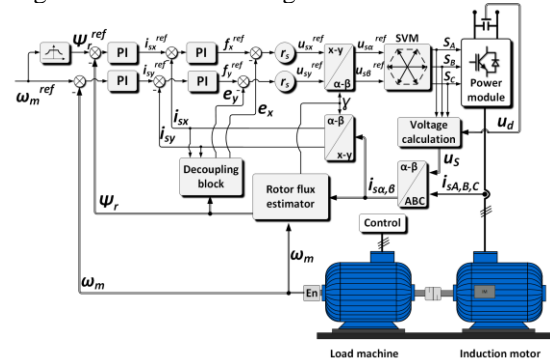


Fig. 2. Vector Control algorithm - DFOC

Presented control structure enable to obtain a good dynamical and steady state performance of the IM. The comprehensive analysis and detailed model of this algorithm have been presented in [14], [43]. A knowledge about the rotor flux vector is crucial to the correct operation of this control system [43]. This state variable can be estimated by the current model (5).

## 3. ESTIMATORS OF INDUCTION MOTOR PARAMETERS BASED ON THE MODEL REFERENCE ADAPTIVE SYSTEMS

In the paper a Flux-error based MRAS (F-MRAS) estimators are used to the rotor and stator resistances calculation. Two separate estimators for

each parameter are applied, but both are based on well-known mathematical models of the rotor flux.

First of them is the Voltage Model (VM) [36], [44]:

$$\frac{d}{dt} \Psi_r^v = \frac{x_r}{x_m T_N} \left( \mathbf{u}_s - r_s \mathbf{i}_s - \sigma x_s T_N \frac{d}{dt} \mathbf{i}_s \right), \quad (14)$$

where:  $\Psi_r^v$  – estimated rotor flux vector by VM,

$$\sigma = 1 - \frac{x_m^2}{x_s x_r}.$$

The second system is the Current Model (CM) [36], [44]:

$$\frac{d}{dt} \Psi_r^i = \frac{1}{T_N} \left( \frac{r_r}{x_r} (x_m \mathbf{i}_s - \Psi_r^i) + j \omega_m \Psi_r^i \right), \quad (15)$$

where:  $\Psi_r^i$  – estimated rotor flux vector by CM.

In further part of this section a detailed models of rotor and stator resistances estimators are presented.

### 3.1. Mathematical Model of the Rotor Windings' Resistance Estimator

To the correct rotor resistance ( $r_r$ ) calculation the estimator proposed in [38] is used. Fig. 3 illustrates the schematic diagram of the mentioned system.

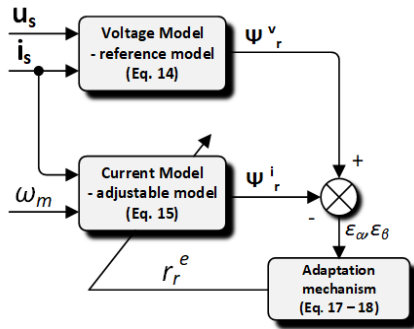


Fig. 3. F-MRAS rotor resistance estimator

The system is divided into two subsystems. Due to dependency on the rotor resistance as an adjustable model the CM is used. The reference model is the VM because it is independent on the rotor resistance value. The estimation algorithm relies on the minimization of the rotor flux error (between VM and CM):

$$\begin{cases} \varepsilon_\alpha = \Psi_{r\alpha}^v - \Psi_{r\alpha}^i \\ \varepsilon_\beta = \Psi_{r\beta}^v - \Psi_{r\beta}^i \end{cases}. \quad (16)$$

Estimated rotor resistance can be obtained from:

$$r_r^{est} = \int A_1 dt + A_2, \quad (17)$$

where:

$$\begin{cases} A_1 = K_1 \left[ \left( \frac{-\Psi_{r\alpha}^i + x_s i_{\alpha s}}{x_r} \right) \varepsilon_\alpha + \left( \frac{-\Psi_{r\beta}^i + x_s i_{\beta s}}{x_r} \right) \varepsilon_\beta \right] \\ A_2 = K_2 \left[ \left( \frac{-\Psi_{r\alpha}^i + x_s i_{\alpha s}}{x_r} \right) \varepsilon_\alpha + \left( \frac{-\Psi_{r\beta}^i + x_s i_{\beta s}}{x_r} \right) \varepsilon_\beta \right] \end{cases}. \quad (18)$$

The adaptation mechanism is based on a PI controller and  $K_1$ ,  $K_2$  are constant coefficients. It is important to point out that the load torque must be applied to estimate the rotor resistance correctly.

### 3.2. Mathematical Model of the Stator Windings' Resistance Estimator

A second system, presented in this chapter, can be used to the stator resistance calculation, which was proposed in [40]. Fig. 4 illustrates scheme of the estimator.

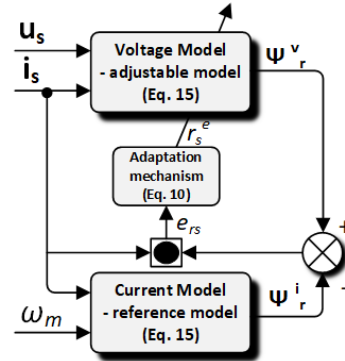


Fig. 4. F-MRAS stator resistance estimator

In this system voltage and current models switch their roles. Due to fact that the CM is independent on the stator resistance it is used as a reference model, while the VM is utilized as an adjustable model. The estimation algorithm is based on the error given by:

$$e_{rs} = i_{s\alpha} (\Psi_{r\alpha}^v - \Psi_{r\alpha}^i) + i_{s\beta} (\Psi_{r\beta}^v - \Psi_{r\beta}^i). \quad (19)$$

The adaptation mechanism is:

$$r_s^{est} = K_{Prs} \left( 1 + \frac{1}{sT_{Irs}} \right) e_{rs}, \quad (20)$$

where:  $K_{Prs}$ ,  $T_{Irs}$  – constant positive coefficients.

It can be easily noticed, that both MRAS estimators are based on the same mathematical models of the rotor flux. Therefore, the rotor resistance estimator is also dependent on the stator resistance, while the stator resistance estimator is dependent on the rotor resistance.

During tests these estimators weren't worked simultaneously, and two assumptions was defined:

- for the rotor resistance estimator - all of IM's parameters (except the rotor resistance) are constant during the drive operation.
- for the stator resistance estimation - all of IM's parameters (except the stator resistance) are constant as well.

It is obvious, that these assumptions are true only in limited range. Windings' temperature has a heavily impact on both resistances' values. Windings faults results in a parameter variation as well (what is presented in this paper). These phenomena can provoke an inaccurate estimation of windings resistances.

To avoid it, an approach based on the universal estimator can be used which has been proposed in [44]. A special mechanism has been described,

which allows to a simultaneous operation of several parameters' estimators.

#### 4. ALGORITHMS FOR THE INDUCTION MOTORS' WINDINGS FAULTS DETECTION

Two winding faults detection algorithms are discussed in the paper. The algorithms cooperate with estimators of windings resistance. A general idea of a detection system is illustrated in Fig. 5. The system is strictly related to the model-based fault detection approach [17], [18].

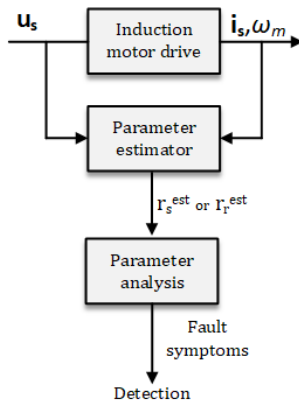


Fig. 5. The main idea of the diagnostic system for IM drive

In the further part of this section a detailed descriptions of detection procedures are presented.

##### 4.1. The rotor fault detection algorithm

The rotor winding faults detection algorithm assumes that ruptures of the rotor bar(s) results in a sharp increase of the estimated rotor resistance. According to the assumption, a simple detection method is proposed which uses a derivative of the estimated rotor resistance:

$$IF \left| \frac{d}{dt} r_r^{est} \right| \geq \varepsilon_{rr} \text{ THEN } 1 \text{ ELSE } 0, \quad (21)$$

where:  $\varepsilon_{rr}$  - threshold of a rotor windings fault detection.

When the modulus of the derivative is greater or equal to the fixed threshold the detector sends a logical 1 which indicates on a bar damage.

##### 4.2. The stator fault detection algorithm

The stator winding faults detection algorithm is analogous to the previous one. It assumes, that ITSC results in a sharp decrease of the estimated stator resistance. Based on this hypothesis, the detection method is proposed, which uses a derivative of the estimated stator resistance:

$$IF \left| \frac{d}{dt} r_s^{est} \right| \geq \varepsilon_{rs} \text{ THEN } 1 \text{ ELSE } 0, \quad (21)$$

where:  $\varepsilon_{rs}$  - threshold of a stator windings fault detection.

If the modulus of the derivative is equal or greater to the threshold the detector sends the logical 1, which indicates on occurring of ITSC.

#### 5. SIMULATION RESULTS

Computer simulation tests were carried out by MATLAB/Simulink software. Table 1 and Table 2 show the IM's rated values and parameters, respectively.

Table 1. Induction motor rated values

$P_N$ [kW]	$U_N$ [V]	$I_N$ [A]	$n_N$ [rpm]	$f_N$ [Hz]	$p_b$ [Hz]
1.1	220/380	5.0/2.9	1400	50	2

Table 2. Induction motor parameters

	$r_s$	$r_r$	$x_s$	$x_r$	$x_m$
[p.u.]	0.1	0.08	1.8	1.8	1.7

Separate tests for each type of windings faults were carried out. Each test was performed for the same conditions: the constant reference speed ( $\omega_{ref} = 0.5\omega_{mN}$ ) as well as constant torque load ( $m_L = 0.5m_N$ ).

Parameters of the IM's from table 2 are presented in the per unit system which detailed description can be found in [43].

##### 5.1. Rotors' windings faults

At first, the rotor fault detection system was verified. A total rupture of rotor bars was modelled (moments of bars cracking, and their amounts are marked on figures as arrows). Fig. 6 shows the transients of the rotor resistance value and signals from the fault detector.

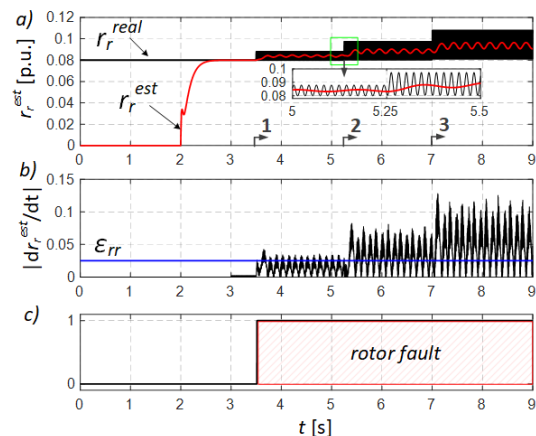


Fig. 6. Rotor winding resistance (a) and detector's signals (b, c) during ruptures of rotor bars; simulation results

It can be observed, that the estimated rotor resistance ( $r_r^{est}$ ) increases according to rotor bars ruptures (Fig. 6a). Consequently, it results in detector activation (Fig. 6b) because the threshold value  $\varepsilon_{rr}$  is exceeded by the modulus of rotor resistance derivative. Ripples in the rotor resistance transient can be observed as well, what is also visible in the detector derivative signal. Fig. 7

presents the transients of the stator current  $i_{sa}$  and stator current component in axis  $y$ .

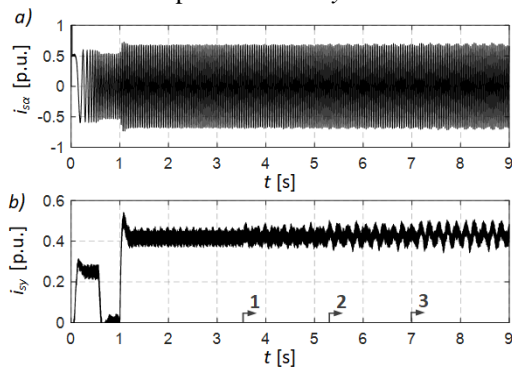


Fig. 7. Stator current components  $i_{sa}$  (a) and  $i_{sy}$  (b) during ruptures of rotor bars; simulation results

It is evident that value of the rotor resistance varies as a result of heating (or cooling) process of machines' windings. It may result in incorrect performance of the fault detector. Therefore, other tests were carried out where a linear increase of the rotor resistance was simulated up to 120% of the nominal value. A low slope of the resistance rise was assumed because of fact, that thermal time constant of the machine can reach even several minutes. Results are shown in Fig. 8 – 9.

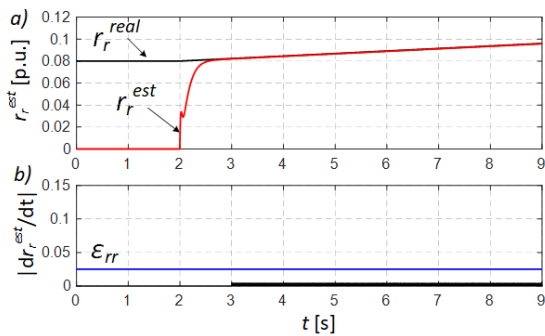


Fig. 8. Rotor winding resistances (a) and detector's signal (b) during heating process; simulation results

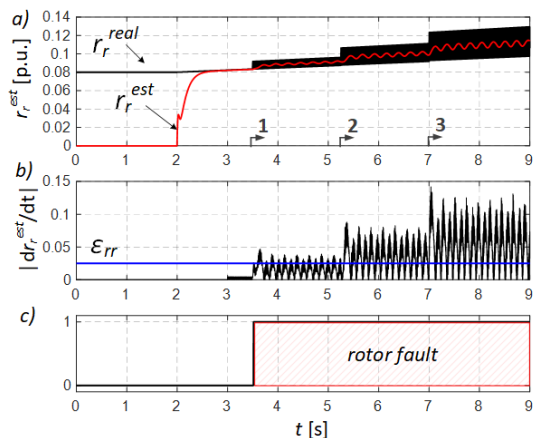


Fig. 9. Rotor winding resistances (a) and detector's signals (b, c) during simultaneous rotors' bars ruptures and heating process; simulation results

It can be noticed, that the derivative value doesn't exceed assumed threshold – variation of rotor resistance due to thermal effects is much slower than due to a bar damage. It can be concluded that proposed rotor fault detector is immune to thermal effects occurring in the machine.

## 5.2. Stators' windings faults

Subsequently, the stator fault detection system was verified. An ITSC in phase A of stator windings were simulated (moments of turns short and their amounts are marked on figures as arrows). Fig. 10 and Fig. 11 shows transients of the estimated stator resistance, signals from fault detector and stator current components.

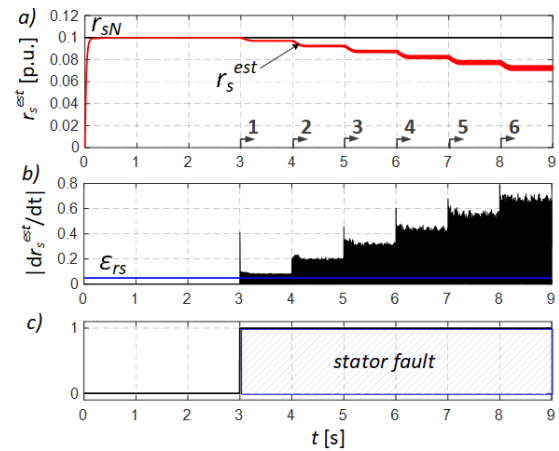


Fig. 10. Stator winding resistance (a) and detector's signals (b, c) during ITCS in phase A; simulation results

It can be observed, that the estimated stator resistance sharply decreases according to short circuits (Fig. 10a). Consequently, it results in the stator's fault detector activation (Fig. 10c) because the threshold value  $\epsilon_{rs}$  is exceeded by the modulus of estimated resistance derivative.

The stator current increases due to ITCS and the amplitude level depends on the fault severity (Fig. 11).

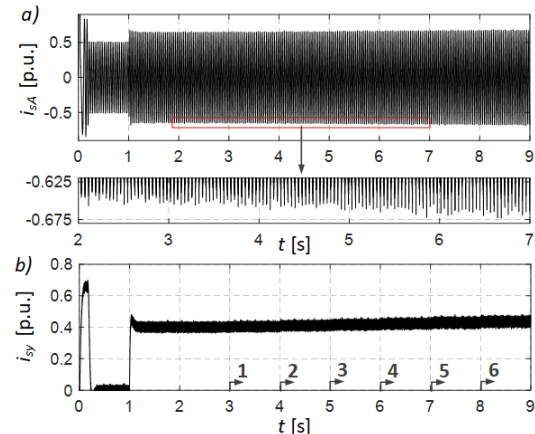


Fig. 11. Stator current in phase A (a) and  $i_{sy}$  current component (b) during ITCS in phase A; simulation results

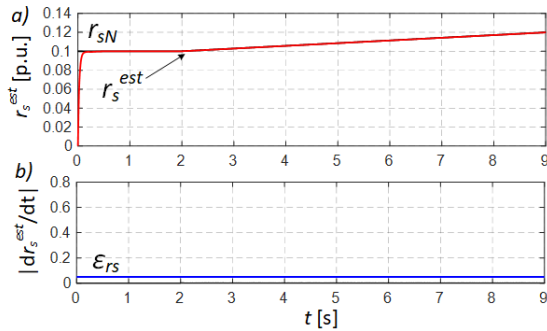


Fig. 12. Stator winding resistance (a) and detector's signal (b) during simultaneous ITSC in phase A and heating process; simulation results

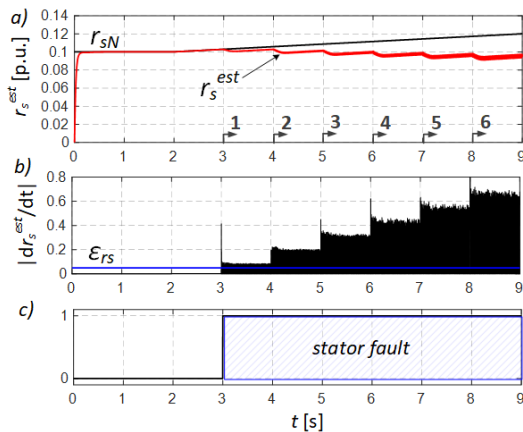


Fig. 13. Stator winding resistance (a) and detector's signals (b, c) during simultaneous ITSC in phase A and heating process; simulation results

Similarly, to the rotor, a value of the stator resistance varies due to heating (or cooling) process of machines' windings. It can provoke incorrect performance of the fault detector as well. Therefore, other tests were performed which were analogous to the case of the rotor faults (a linear increase of the stator resistance were simulated up to 120% of the nominal value).

In Fig. 12 it can be noticed, that derivative value doesn't exceed assumed threshold. It can be concluded, that proposed stator fault detector is also immune to thermal effects which are occurred in the machine.

## 6. EXPERIMENTAL RESULTS

To validate proposed systems in practice experimental tests were performed using a laboratory setup (Fig.14). The setup is equipped with the induction machine with special prepared terminal box what enable to conduct controlled ITSC in each phase of the stator windings. Additionally, the laboratory setup has a set of squirrel-cage rotors with cracked bars. The IM which is used to faults modelling is supplied by inverter controlled using rapid prototyping system DS1103 by dSPACE. The load machine is controlled by another inverter.

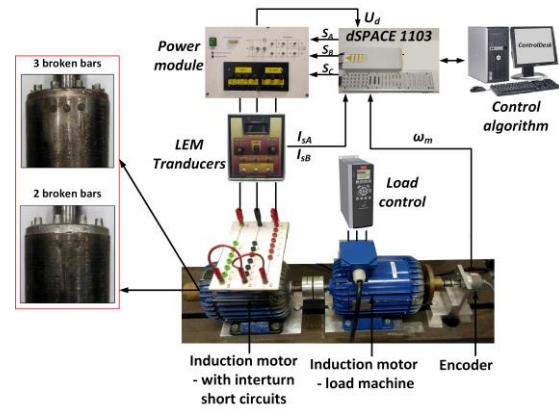


Fig. 14. Diagram in the laboratory setup

Separate experimental tests for each type of windings faults were carried out. Each test was performed for the same conditions: the constant reference speed ( $\omega_{ref} = 0.5\omega_{mN}$ ) as well as constant torque load ( $m_L = 0.25m_N$ ).

### 6.1. Rotor windings faults

At first, the rotor fault detection system was verified. The parameter identification algorithm was applied at  $t=2s$ .

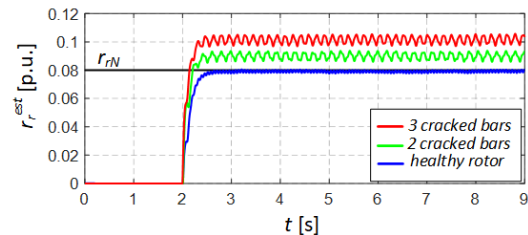


Fig. 15. Estimated rotor winding resistances for healthy and faulted rotor; experimental results

Fig. 15 shows a comparison of estimated rotor resistances for the healthy and the faulted rotor. It can be seen easily, that the rotor resistance increases due to the bar(s) rupture(s). Amplitudes of oscillations of estimated rotor resistance transients rise as well.

Afterwards the rotor fault detection algorithm was turned on (at  $t=3s$ ). In Fig. 16 it can be observed, that the fault detection threshold is exceeded only for faulty scenarios, so the system behaves appropriately. The  $\epsilon_{rr}$  threshold value was fixed as 0.15 for the experimental test. It can be seen also that a difference between derivative values for 2 and 3 broken bars isn't very relevant.

Furthermore, transients of the stator  $i_{s\alpha}$  and  $i_{s\beta}$  components, for healthy and faulted conditions on the rotor's winding are presented in Fig. 17. For two cracked bars, each of presented signal characterized by oscillations, which may have negative impact on the drives' performance.

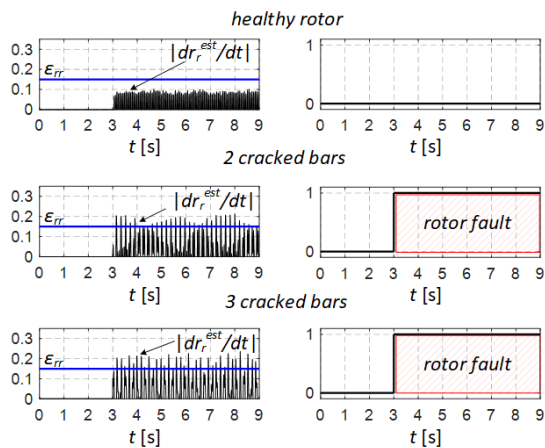


Fig. 16. Comparison of detector's signals for healthy and faulted rotor; experimental results

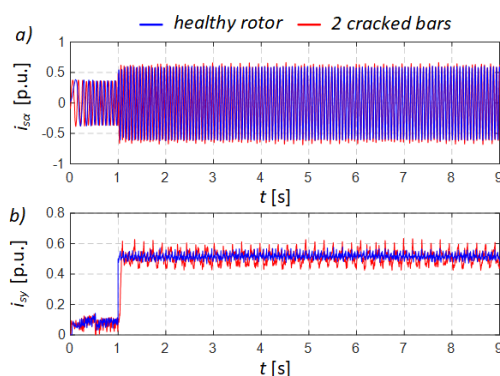


Fig. 17. Stator  $i_{sa}$  (a) and  $i_{sy}$  (b) current components for healthy and faulted rotor; experimental results

## 6.2. Stator windings faults

Next the experimental validation of stator fault detection system was carried out. The system was tested for 2, 3, 5 and 7 shorted turns in phase A. It can be observed a sharp decrease of the estimated stator resistance value due to ITCS (Fig 18).

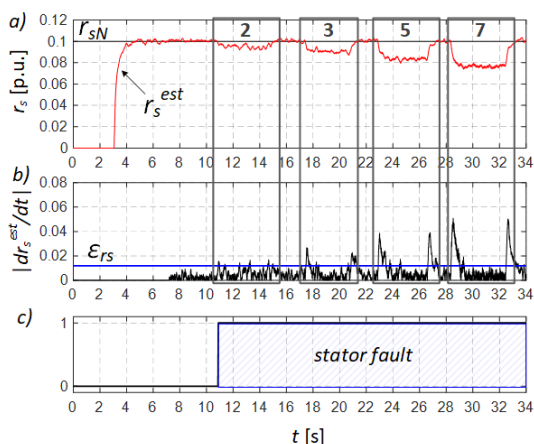


Fig. 18. Stator winding resistance (a) and detector's signals (b, c) during ITCS in phase A; experimental results

It results in an increase of the derivative value and consequently in activation of the stator fault detector. Fig. 19 shows an impact of the ITCS on

the stator currents transients. An increase of the  $i_{sa}$  amplitude and  $i_{sy}$  value is noticeable.

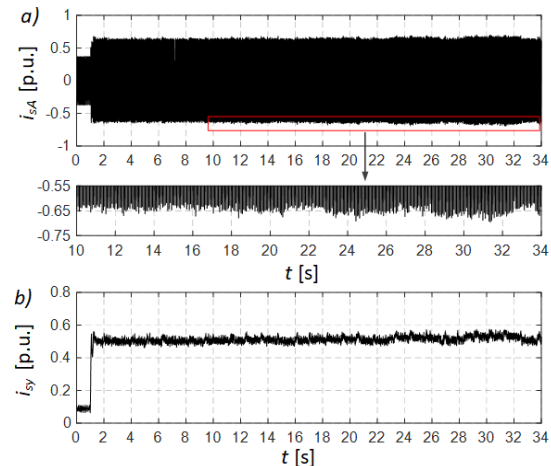


Fig. 19 Stator current in phase A (a) and  $i_{sy}$  current component (b) during ITSC in phase A; experimental results

## 7. CONCLUSIONS

In the paper two systems for IM fault detection were proposed. The first one for the rotor's bars cracking detection and the second one for ITSC detection in stator windings. Both systems rely on the hypothesis that each of windings faults results in a sharp change of internal parameters' values of the motor, thus observation and analysis of changes these parameters in a enable to faults detection. Therefore, estimators of IM parameters based on MRAS technique are used to calculate rotor and stator resistances. Obtained resistances are utilized in simple detection algorithms which are based on derivative calculation. Both systems are described in detail. The data gathered in the simulation and experimental studies are convergent what confirm usefulness of proposed systems.

The main feature of both systems is quite simplicity in implementation because they utilized a well-know mathematical model of the IM and derivative algorithm. Moreover, to enable proper operation of the vector control method an on-line identification of the machine's parameters should be applied, nevertheless. On the other hand, MRAS estimators are dependent not only on calculated parameter what is the main problem, but It can be solved by methods mentioned in the paper.

## REFERENCES

1. Bose BK. Power electronics and motor drives: advances and trends. Elsevier; 2006.
2. Campos-Delgado DU, Espinoza-Trejo DR, Palacios E. Fault-tolerant control in variable speed drives: a survey. IET Electric Power Applications. 2008; 2(2): 121–134. <http://dx.doi.org/10.1049/iet-epa:20070203>
3. Riera-Guasp M, Antonino-Daviu JA, Capolino GA. Advances in Electrical Machine, Power Electronic, and Drive Condition Monitoring and Fault Detection: State of the Art. IEEE Transactions on Industrial

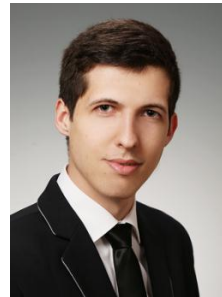
- Electronics. 2015; 62(3): 1746–1759. <http://dx.doi.org/10.1109/TIE.2014.2375853>
4. Bellini A, Filippetti F, Tassoni C, Capolino GA. Advances in Diagnostic Techniques for Induction Machines. IEEE Transactions on Industrial Electronics. 2008; 55(12): 4109–4126. <http://dx.doi.org/10.1109/TIE.2008.2007527>
  5. Zhang P, Du Y, Habetler TG, Lu B. A Survey of Condition Monitoring and Protection Methods for Medium-Voltage Induction Motors. IEEE Transactions on Industry Applications. 2010; 47(1): 34–46. <http://dx.doi.org/10.1109/TIA.2010.2090839>
  6. Gandhi A, Corrigan T, Parsa L. Recent Advances in Modeling and Online Detection of Stator Interturn Faults in Electrical Motors. IEEE Transactions on Industrial Electronics. 2010; 58(5): 1564–1575. <http://dx.doi.org/10.1109/TIE.2010.2089937>
  7. Siddique A, Yadava GS, Singh B. A review of stator fault monitoring techniques of induction motors. IEEE Transactions on Energy Conversion. 2005;20(1):106–14. <http://dx.doi.org/10.1109/TEC.2004.837304>
  8. Ewert P. Application of neural networks and axial flux for the stator and rotor fault detection of induction motor. Power Electronics and Drives. 2018;1–13. <https://doi.org/10.2478/pead-2019-0001>
  9. Bellini A, Filippetti F, Franceschini G, Tassoni C. Closed-loop control impact on the diagnosis of induction motors faults. IEEE Transactions on Industry Applications. 2000;36(5):1318–29. <http://dx.doi.org/10.1109/28.871280>
  10. Cheng S, Zhang P, Habetler TG. An impedance identification approach to sensitive detection and location of stator turn-to-turn faults in a closed-loop multiple-motor drive. IEEE Transactions on Industrial Electronics. 2011;58(5):1545–54. <http://dx.doi.org/10.1109/TIE.2010.2064276>
  11. Tallam RM, Habetler TG, Harley RG. Stator winding turn-fault detection for closed-loop induction motor drives. IEEE Transactions on Industry Applications. 2003; 39(3):1553–7. <http://dx.doi.org/10.1109/TIA.2003.811784>
  12. Cruz SMA, Cardoso AJM. Diagnosis of Stator Inter-Turn Short Circuits in DTC Induction Motor Drives. IEEE Transactions on Industry Applications. 2004; 40(5):1349–60. <http://dx.doi.org/10.1109/TIA.2004.834012>
  13. Cruz SMA, Cardoso AJM. Fault Indicators for the Diagnosis of Rotor Faults in FOC Induction Motor Drives. In: 2007 IEEE International Electric Machines & Drives Conference; 1136–41. <http://dx.doi.org/10.1109/IEMDC.2007.383590>
  14. Wolkiewicz M, Tarchała G, Orłowska-Kowalska T, Kowalski CT. Online Stator Interturn Short Circuits Monitoring in the DFOC Induction-Motor Drive. IEEE Transactions on Industrial Electronics. 2016;63(4):2517–28. <http://dx.doi.org/10.1109/TIE.2016.2520902>
  15. Wolkiewicz M, Tarchała G, Kowalski T, Orłowska-Kowalska T. Advanced Control of Electrical Drives and Power Electronic Converters. 2017; 75:169-191. <http://dx.doi.org/10.1007/978-3-319-45735-2>
  16. Wolkiewicz M, Tarchała G, Orłowska-Kowalska T. Diagnosis of stator and rotor faults of an induction motor in closed-loop control structure. In: 2018 International Symposium on Power Electronics, Electrical Drives, Automation and Motion (SPEEDAM); 2018. 196–201. <http://dx.doi.org/10.1109/SPEEDAM.2018.8445282>
  17. Iserman R. Fault-Diagnosis Applications, Model-Based Condition Monitoring: Actuators, Drives, Machinery, Plants, Sensors, and Fault-tolerant Systems. Springer-Verlag Berlin Heidelberg; 2011. <https://dx.doi.org/10.1007/978-3-642-12767-0>
  18. Gao Z, Cecati C, Ding SX. A Survey of Fault Diagnosis and Fault-Tolerant Techniques—Part I: Fault Diagnosis with Model-Based and Signal-Based Approaches. IEEE Transactions on Industrial Electronics. 2015;62(6):3757–67. <http://dx.doi.org/10.1109/TIE.2015.2417501>
  19. Cho KR, Lang JH, Umans SD. Detection of broken rotor bars in induction motors using state and parameter estimation. IEEE Transactions on Industry Applications. 1992;28(3):702–709. <http://dx.doi.org/10.1109/28.137460>
  20. Bachir S, Tnani S, Trigeassou JC, Champenois G. Diagnosis by parameter estimation of stator and rotor faults occurring in induction machines. IEEE Transactions on Industrial Electronics. 2006; 53(3):963–73. <http://dx.doi.org/10.1109/TIE.2006.874258>
  21. Said MSN, Benbouzid MEH, Benchaib A. Detection of broken bars in induction motors using an extended Kalman filter for rotor resistance sensorless estimation. IEEE Transactions on Energy Conversion. 2000;15(1):66–70. <http://dx.doi.org/10.1109/60.849118>
  22. Bachir S, Trigeassou JC, Tnani S. On-Line Stator Faults Diagnosis By Parameter Estimation. In: European Conference on Power Electronics and Applications (EPE); 2003. p. 209–19.
  23. Kowalski CT, Wierzbicki R, Wolkiewicz M. Stator and Rotor Faults Monitoring of the Inverter-Fed Induction Motor Drive using State Estimators. Automatika. 2013;54(3):348–55. <http://dx.doi.org/10.7305/automatika.54-3.167>
  24. Bazine IBA, Tnani S, Poinot T, Champenois G, Jelassi K. On-line detection of stator and rotor faults occurring in induction machine diagnosis by parameters estimation. In: 8th IEEE Symposium on Diagnostics for Electrical Machines, Power Electronics & Drives; 2011: 105–12. <http://dx.doi.org/10.1109/DEMPED.2011.6063609>
  25. Karami F, Poshtan J, Poshtan M. Detection of broken rotor bars in induction motors using nonlinear Kalman filters. ISA Transactions. 2010;49(2):189–95. <http://dx.doi.org/10.1016/j.isatra.2009.11.005>
  26. Nguyen V, Wang D, Seshadrinath J, Nadarajan S, Vaiyapuri V. Fault severity estimation using nonlinear Kalman filter for induction motors under inter-turn fault. In: 42nd Annual Conference of the IEEE Industrial Electronics Society (IECON); 2016: 1488–93. <http://dx.doi.org/10.1109/IECON.2016.7792962>
  27. Nguyen V, Wang D, Seshadrinath J, Ukil A, Krishna MS, Nadarajan S. A Method for Incipient Interturn Fault Detection and Severity Estimation of Induction Motors Under Inherent Asymmetry and Voltage Imbalance. IEEE Transactions on Transportation Electrification. 2017;3(3):703–15. <http://dx.doi.org/10.1109/TTE.2017.2726351>
  28. Kallesøe CS, Izadi-Zamanabadi R, Vadstrup PP, Rasmussen H. Observer-based estimation of stator-winding faults in delta-connected induction motors: A linear matrix inequality approach. IEEE

- Transactions on Industry Applications. 2007;43(4):1022–31.  
<http://dx.doi.org/10.1109/TIA.2007.900494>
29. De Angelo CH, Bossio GR, Giaccone SJ, Valla MI, Solsona JA, Garcia GO. Online Model-Based Stator-Fault Detection and Identification in Induction Motors. *IEEE Transactions on Industrial Electronics*. 2009;56(11):4671–80.  
<http://dx.doi.org/10.1109/TIE.2009.2012468>
30. Abdallah H, Benatman K. Stator winding inter-turn short-circuit detection in induction motors by parameter identification. *IET Electric Power Applications*. 2017;11(2):272–88.  
<http://dx.doi.org/10.1049/iet-epa.2016.0432>
31. Chouiref H, Boussaid B, Abdelkrim MN, Aubrun C. Nonlinear fault tolerant control-based parameter estimation diagnosis: Application to induction motors. In: 10th International Multi-Conferences on Systems, Signals & Devices (SSD); 2013:1–6.  
<http://dx.doi.org/10.1109/SSD.2013.6564118>
32. Tretrong J. Electric Motor Fault Diagnosis Based on Parameter Estimation Approach Using Genetic Algorithm. In: International Multi Conference of Engineers and Computer Scientist (IMECS); 2010.
33. Duan F, Zivanovic R. Condition Monitoring of an Induction Motor Stator Windings Via Global Optimization Based on the Hyperbolic Cross Points. *IEEE Transactions on Industrial Electronics*. 2015;62(3):1826–34.  
<http://dx.doi.org/10.1109/TIE.2014.2341563>
34. Sellami T, Berriri H, Jelassi S, Mimouni MF. Sliding mode observer-based fault-detection of inter-turn short-circuit in induction motor. In: 14th International Conference on Sciences and Techniques of Automatic Control & Computer Engineering - STA'2013; 2013:524–529.  
<http://dx.doi.org/10.1109/STA.2013.6783182>
35. Toliyat HA, Levi E, Raina M. A review of RFO induction motor parameter estimation techniques. *IEEE Transactions on Energy Conversion*. 2003;18(2):271–83.  
<http://dx.doi.org/10.1109/TEC.2003.811719>
36. Syam P, Kumar R, Das S, Chattopadhyay AK. Review on model reference adaptive system for sensorless vector control of induction motor drives. *IET Electric Power Applications*. 2015;9(7):496–511.  
<http://dx.doi.org/10.1049/iet-epa.2014.0220>
37. Zorgani Y, Jouili M, Koubaa Y. A very low speed sensorless control induction motor drive with online rotor resistance using MRAS Scheme. *Power Electronics and Drives*. 2018;3(38):171–186.  
<https://doi.org/10.2478/pead-2018-0021>
38. Zorgani YA, Koubaa Y, Boussak M. Sensorless speed control with MRAS for induction motor drive. In: XXth International Conference on Electrical Machines (ICEM); 2012:2259–65.  
<http://dx.doi.org/10.1109/ICEIMach.2012.6350196>
39. Bednarz SA, Dybkowski M. On-line detection of the rotor faults in the induction motor drive using parameter estimator. In: 2018 International Symposium on Electrical Machines (SME); 2018. p. 1–5.  
<http://dx.doi.org/10.1109/ISEM.2018.8443020>
40. Vasic V, Vukosavic SN, Levi E. A stator resistance estimation scheme for speed sensorless rotor flux-oriented induction motor drives. *IEEE Trans Energy Convers*. 2003 Dec;18(4):476–83.  
<http://dx.doi.org/10.1109/TEC.2003.816595>
41. Bednarz SA, Dybkowski M, Wolkiewicz M. Identification of the Stator Faults in the Induction Motor Drives Using Parameter Estimator. In: *IEEE 18th International Power Electronics and Motion Control Conference (PEMC)*; 2018. p. 688–93.  
<http://dx.doi.org/10.1109/EPEPMC.2018.8521893>
42. Pawlak M, Orłowska-Kowalska T. Application of the simplified two axial model for rotor faults modeling of the induction motor. *Przegląd Elektrotechniczny*. 2006;82(10):48–53. Polish.
43. Kaźmierkowski MP, Krishnan R, Blaabjerg F. *Control in power electronics: selected problems*. Elsevier; 2003.
44. Dybkowski M. *Universal Speed and Flux Estimator for Induction Motor*. *Power Electron Drives*. 2018;3(1):157–69.  
<http://dx.doi.org/10.2478/pead-2018-0007>

Received 2019-02-12

Accepted 2019-04-30

Available online 2019-05-10



**Szymon BEDNARZ** received the M.Sc. degree from the Faculty of Electrical Engineering, Wrocław University of Science and Technology, Wrocław, Poland, in 2017. Since October 2017 he has been a PhD student in electrical engineering in Department of Electrical Machines, Drives and Measurements. His main research interests include control structures for induction motor, state variables and parameters estimation, diagnostics, and fault-tolerant control techniques.



**Mateusz DYBKOWSKI** received M.S., and Ph. D degrees in Electrical Engineering in Wrocław University of Technology, Poland, in 2004, 2008 respectively. In 2014 he received D.Sc. (Habilitation) on the Electrical Engineering Faculty of the Wrocław University of Technology. Since 2015 he is a professor in the Department of Electrical Engineering. His major research fields are the sensorless drives system, fault tolerant control systems, state and variable estimation, traction drives systems, e-mobility and Power Electronics in Electrical Drives. He is a Deputy Editor-in-Chief in *Power Electronics and Drives* journal and head of the Laboratory of Industrial Automation.